DE LA RECHERCHE À L'INDUSTRIE

Technical Meeting on Compilation Of Nuclear Data Experiments for Radiation Characterization

October, 10th - 14th 2022

Analysis of the FNS-Duct experiment with the Monte Carlo code TRIPOLI-4®

IRFM/SI²P/GISP

IRFM/SI²P/GISP

Institut de Recherche sur la Fusion par confinement Magnétique

Scope

Previous work performed in the framework of a collaboration with an ASIPP engineer revisited for the CONDERC Technical Meeting

- TRIPOLI-4® training
- Application to a benchmark before applying to CFETR analysis

New TRIPOLI-4® release

New nuclear data libraries

New benchmark model

New Variance Reduction Techniques

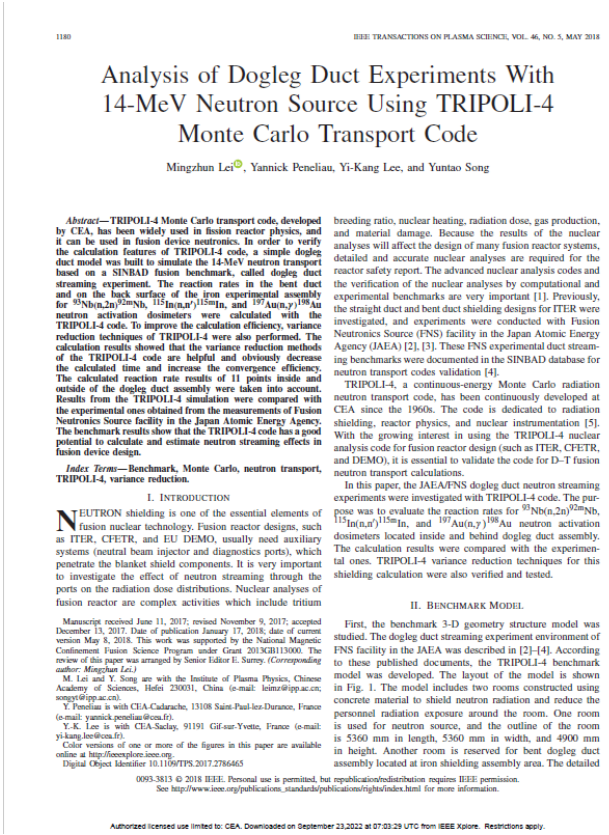

1180 IEEE TRANSACTIONS ON PLASMA SCIENCE, VOL. 46, NO. 5, MAY 2018

Analysis of Dogleg Duct Experiments With 14-MeV Neutron Source Using TRIPOLI-4 Monte Carlo Transport Code

Mingzhun Lei, Yannick Peneliau, Yi-Kang Lee, and Yuntao Song

***Abstract*—TRIPOLI-4 Monte Carlo transport code, developed by CEA, has been widely used in fission reactor physics, and it can be used in fusion device neutronics. In order to verify the calculation features of TRIPOLI-4 code, a simple dogleg duct model was built to simulate the 14-MeV neutron transport based on a SINBAD fusion benchmark, called dogleg duct streaming experiment. The reaction rates in the bent duct and on the back surface of the iron experimental assembly for ^{93}Nb(n,2n)^{92m}Nb, ^{115}In(n,n')^{115m}In, and ^{197}Au(n,γ)^{198}Au neutron activation dosimeters were calculated with the TRIPOLI-4 code. To improve the calculation efficiency, variance reduction techniques of TRIPOLI-4 were also performed. The calculation results showed that the variance reduction methods of the TRIPOLI-4 code are helpful and obviously decrease the calculated time and increase the convergence efficiency. The calculated reaction rate results of 11 points inside and outside of the dogleg duct assembly were taken into account. Results from the TRIPOLI-4 simulation were compared with the experimental ones obtained from the measurements of Fusion Neutronics Source facility in the Japan Atomic Energy Agency. The benchmark results show that the TRIPOLI-4 code has a good potential to calculate and estimate neutron streaming effects in fusion device design.**

***Index Terms*—Benchmark, Monte Carlo, neutron transport, TRIPOLI-4, variance reduction.**

I. Introduction

NEUTRON shielding is one of the essential elements of fusion nuclear technology. Fusion reactor designs, such as ITER, CFETR, and EU DEMO, usually need auxiliary systems (neutral beam injector and diagnostics ports), which penetrate the blanket shield components. It is very important to investigate the effect of neutron streaming through the ports on the radiation dose distributions. Nuclear analyses of fusion reactor are complex activities which include tritium breeding ratio, nuclear heating, radiation dose, gas production, and material damage. Because the results of the nuclear analyses will affect the design of many fusion reactor systems, detailed and accurate nuclear analyses are required for the reactor safety report. The advanced nuclear analysis codes and the verification of the nuclear analyses by computational and experimental benchmarks are very important [1]. Previously, the straight duct and bent duct shielding designs for ITER were investigated, and experiments were conducted with Fusion Neutronics Source (FNS) facility in the Japan Atomic Energy Agency (JAEA) [2], [3]. These FNS experimental duct streaming benchmarks were documented in the SINBAD database for neutron transport codes validation [4].

TRIPOLI-4, a continuous-energy Monte Carlo radiation neutron transport code, has been continuously developed at CEA since the 1960s. The code is dedicated to radiation shielding, reactor physics, and nuclear instrumentation [5]. With the growing interest in using the TRIPOLI-4 nuclear analysis code for fusion reactor design (such as ITER, CFETR, and DEMO), it is essential to validate the code for D–T fusion neutron transport calculations.

In this paper, the JAEA/FNS dogleg duct neutron streaming experiments were investigated with TRIPOLI-4 code. The purpose was to evaluate the reaction rates for ^{93}Nb(n,2n)^{92m}Nb, ^{115}In(n,n')^{115m}In, and ^{197}Au(n,γ)^{198}Au neutron activation dosimeters located inside and behind dogleg duct assembly. The calculation results were compared with the experimental ones. TRIPOLI-4 variance reduction techniques for this shielding calculation were also verified and tested.

II. Benchmark Model

First, the benchmark 3-D geometry structure model was studied. The dogleg duct streaming experiment environment of FNS facility in the JAEA was described in [2]–[4]. According to these published documents, the TRIPOLI-4 benchmark model was developed. The layout of the model is shown in Fig. 1. The model includes two rooms constructed using concrete material to shield neutron radiation and reduce the personnel radiation exposure around the room. One room is used for neutron source, and the outline of the room is 5360 mm in length, 5360 mm in width, and 4900 mm in height. Another room is reserved for bent dogleg duct assembly located at iron shielding assembly area. The detailed

Manuscript received June 11, 2017; revised November 9, 2017; accepted December 13, 2017. Date of publication January 17, 2018; date of current version May 8, 2018. This work was supported by the National Magnetic Confinement Fusion Science Program under Grant 2013GB113000. The review of this paper was arranged by Senior Editor E. Surrey. *(Corresponding author: Mingzhun Lei.)*

M. Lei and Y. Song are with the Institute of Plasma Physics, Chinese Academy of Sciences, Hefei 230031, China (e-mail: leimz@ipp.ac.cn; songyt@ipp.ac.cn).

Y. Peneliau is with CEA-Cadarache, 13108 Saint-Paul-lez-Durance, France (e-mail: yannick.peneliau@cea.fr).

Y.-K. Lee is with CEA-Saclay, 91191 Gif-sur-Yvette, France (e-mail: yi-kang.lee@cea.fr).

Color versions of one or more of the figures in this paper are available online at http://ieeexplore.ieee.org.

Digital Object Identifier 10.1109/TPS.2017.2786465

Benchmark interest

The dogleg is a typical shielding design in diagnostics or NBI ports in fusion reactors

- Monitoring of the reactor (plasma facing components)
- Ray or any other signal transmission through paths (streaming paths for neutron and photons)
- Signal processing further

Validation of particle transport in dogleg is of utmost importance for the Monte Carlo codes

- Diffusion cross sections
- Anisotropy (elastic diffusion, inelastic diffusion)

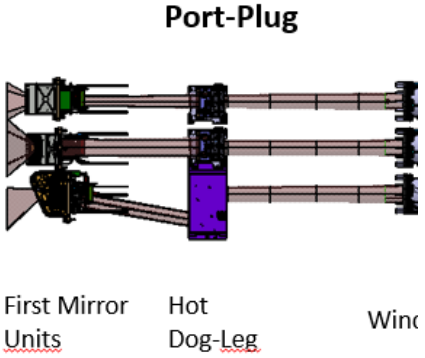

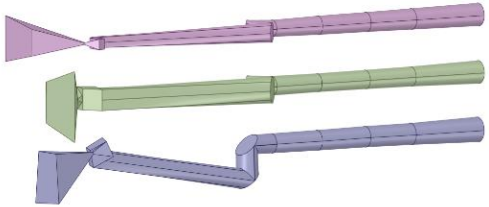

Vis IR WAVS diagnostic design in Port Plug part

Outline

FNS Duct Experiment

TRIPOLI-4® model

Nuclear data

Variance reduction techniques

Results and discussion

DE LA RECHERCHE À L'INDUSTRIE

Experiment

IRFM/SI²P/GISP

Institut de Recherche sur la Fusion par confinement Magnétique

Experiment presentation

- Fusion Neutronics Source at JAERI dedicated to Fusion experiments
- DT 14 MeV neutron source → 4 10^{12} n/s
- Doubly bent duct in iron assembly
- Rotating neutron source, irradiation room, experimental room

An irradiation room (or target rool)

Neutron source room 536 cm length, 536 cm width, 490 cm height

An experiment room

2004 experiment

ITER interest: dogleg in diagnostics (instrumentation/detector)

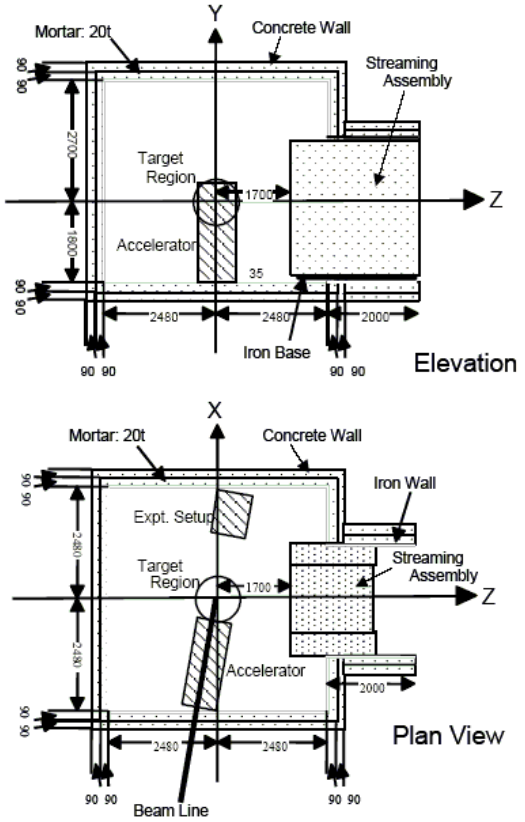

Fig.1 Layout of the target room.

Experimental setup

Streaming assembly in iron

170 cm (high) X 140 cm (wide) x 180 cm (thick)

Auxiliary shield: iron and PolyEthylene (PE)

Streaming assembly: iron

Streaming duct

30 cm x 30 cm and 115 cm length for the 1st leg, 60 for the 2nd leg and 65 cm for the 3rd leg

Main materials

- Auxiliary shield made of iron: ρ = 6.46 g/cc

Mixture of PolyEthylene and Pure iron (around 20%$_{vol}$ – 80%$_{vol}$)

- Streaming assembly: ρ = 7.83 g/cc

Pure iron with C, Si, P, S, Mn impurities

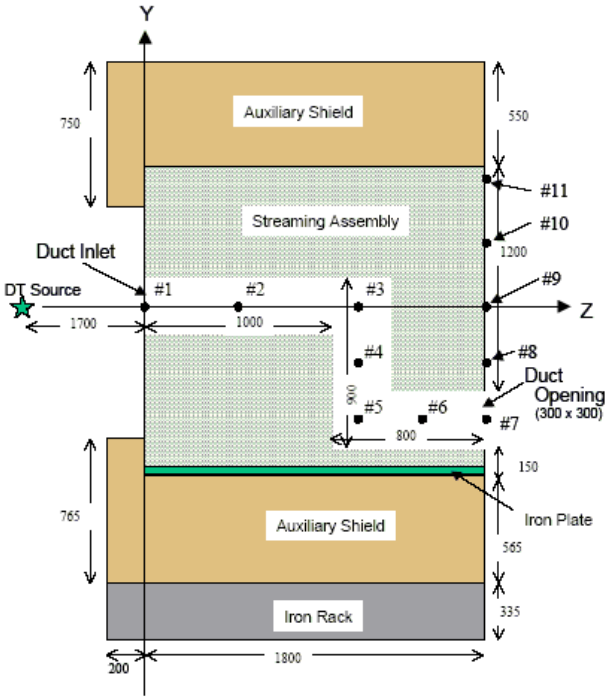

Fig.2 Schematic view of the experimental assembly.

Neutron source

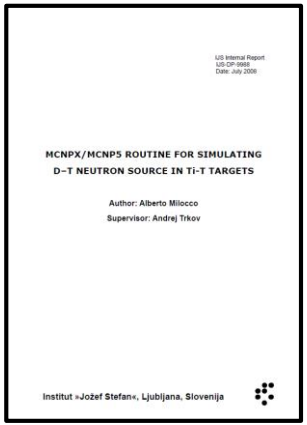
US Internal Report
US-DP-9988
Date: July 2006

MCNPX/MCNP5 ROUTINE FOR SIMULATING D–T NEUTRON SOURCE IN Ti-T TARGETS

Author: Alberto Milocco
Supervisor: Andrej Trkov

Institut »Jožef Stefan«, Ljubljana, Slovenija

DT 14 MeV neutron source → 4 10^{12} n/s

- **Deuteron beam** ——— hitting a titanium hydride target (with ^{3}H = T) producing 14 MeV fusion neutrons

A dedicated source subroutine for MCNP-5 developed to implement:

- Slowing down of the deuterons in the Ti-T target
- Kinematics of the $^{3}T(d, n)^{4}HE$ reaction
- Neutron production

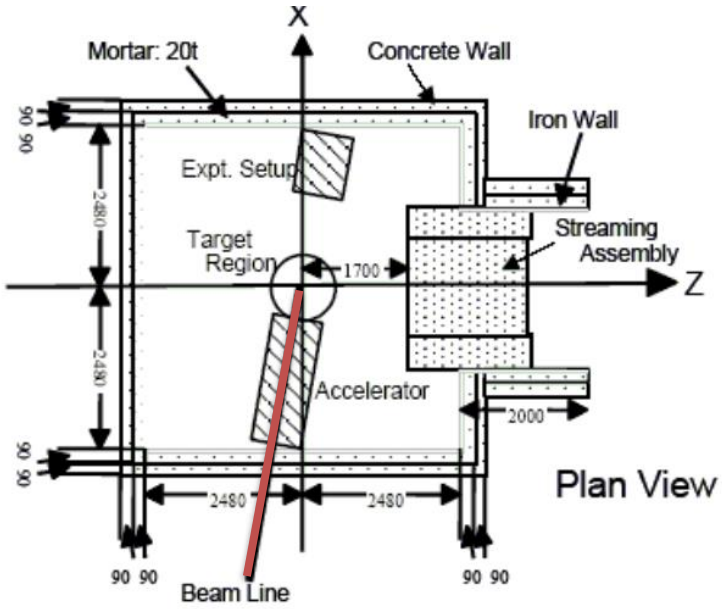

Source subroutine validated through the FNS experiments and analyses

Measurements

Measurements

- Activation foils and reaction rates

^{93}Nb (n, 2n) ^{92m}Nb	E_{th} = 8.9 MeV
^{115}In (n, n') ^{115m}In	E_{th} = 0.3 MeV
^{197}Au (n, γ) ^{198}Au	No threshold

No information provided on the foil geometry

11 detectors in the duct: #1 #2 #3 in the 1st leg

#4, #5 in the 2nd leg, #6, #7 in the 3rd leg, #8, #9, #10, #11 behind

- Neutron flux spectra at locations #3, #5, #7, #9 with a NE213 scintillation spectrometer

  Neutron and gamma rays separated thanks to the difference in the rise time of the signal (pulse mode)

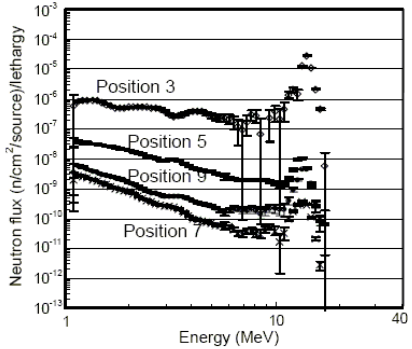

Fig.3 Neutron spectra measured at positions #3, #5, #7 and #9.

Neutron spectra become softer along the duct

Position #9 flux is higher than #7 because it is in front of the 1st leg

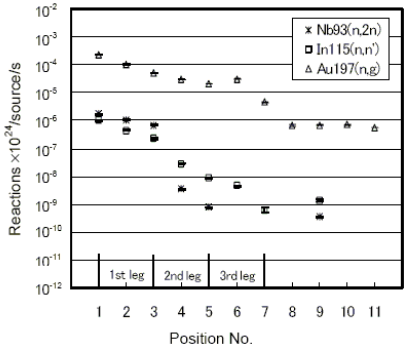

Fig.4 Reaction rates measured in the duct and behind the assembly.

^{93}Nb(n, 2n) and ^{115}In(n, n') attenuation is larger than ^{197}Au(n, γ)

Benchmark description

Benchmark quality discussion:

- **Intermediate** quality from SINBAD assessment
- Neutron source spectrum
- Experimantal energy calibration
- Neutron detector response function

Data provision

- MCNP-5 data file with appropriate source definition (RDUM card)
- Documentation describing 1) the quality assessment and 2) the DT source routine to use in MCNP-5
- DT_MCNP5.TXT patch file (to apply for MCNP-5 compilation)
- Experimental results in HTML and XLS files

DOGLEG DUCT EXPERIMENT		EXP	MCNPX(5)
GEOMETRY	SAMPLE	♦♦♦	♦♦♦
	SHIELD	♦♦♦	♦♦♦
	RACK	♦♦♦	♦♦♦
	BEAM TUBE	♦♦	♦♦
	TARGET PLATE	♦♦	♦♦
	TARGET BACKING	♦♦	♦♦
	TARGET COOLING SYSTEM	♦	♦
	FLANGE	♦	♦
	NEUTRON DETECTOR	♦♦♦	♦♦
	ACTIVATION FOILS	♦♦	♦♦
	N. DETECTOR HOUSING	♦	♦
	A. FOILS HOUSING	♦	♦
	ROOM WALLS	♦♦♦	♦♦♦
MATERIALS	SAMPLE	♦♦♦	♦♦♦
	SHIELD	♦♦♦	♦♦♦
	RACK	♦♦♦	♦♦♦
	BEAM TUBE	♦♦	♦♦
	TARGET PLATE	♦♦	♦♦
	TARGET BACKING	♦♦	♦♦
	TARGET COOLING SYSTEM	♦	♦
	FLANGE	♦	♦
	NEUTRON DETECTOR	♦♦	♦
	ACTIVATION FOILS	♦♦	♦
	N. DETECTOR HOUSING	♦	♦
	A. FOILS HOUSING	♦	♦
	ROOM WALLS	♦♦♦	♦♦♦
	AIR	♦♦♦	♦♦♦
SOURCE	SOURCE ROUTINE	♦♦	♦♦
	ENERGY SPECTRUM	♦	♦
	ANISOTROPY YIELDS	♦	♦
	ANISOTROPY EN. DISCRETE	♦	♦
	ANISOTROPY EN. SPECTRUM	♦	♦
SIGNAL	NEUTRON FLUX CELL	♦♦♦	♦♦♦
	NEUTRON FLUX SURFACE	♦♦	♦
	REACTION RATES CELL	♦♦♦	♦♦♦
	REACTION RATES SURFACE	♦♦	♦
	BACKGROUND	♦	♦

Table III.a–4. Quantitative quality assessment of the experimental specifications and relative features included in the MCNP5 models

DE LA RECHERCHE À L'INDUSTRIE

TRIPOLI-4® model

IRFM/SI²P/GISP

Institut de Recherche sur la Fusion par confinement Magnétique

Geometrical model

Conversion thanks to t4_geom_convert tool from the MCNP-5 data file

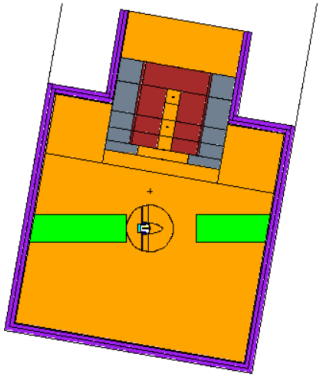

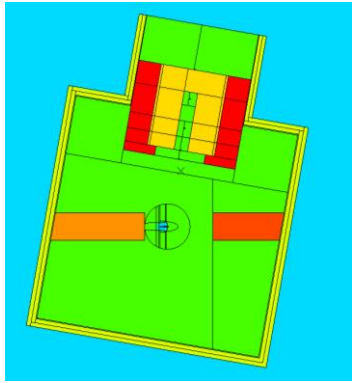

A powerfull tool for processing MCNP-5/6 data files into TRIPOLI-4® data files

- Cross checking, TRIPOLI-4® testing

Irradiation and assembly rooms

X=0

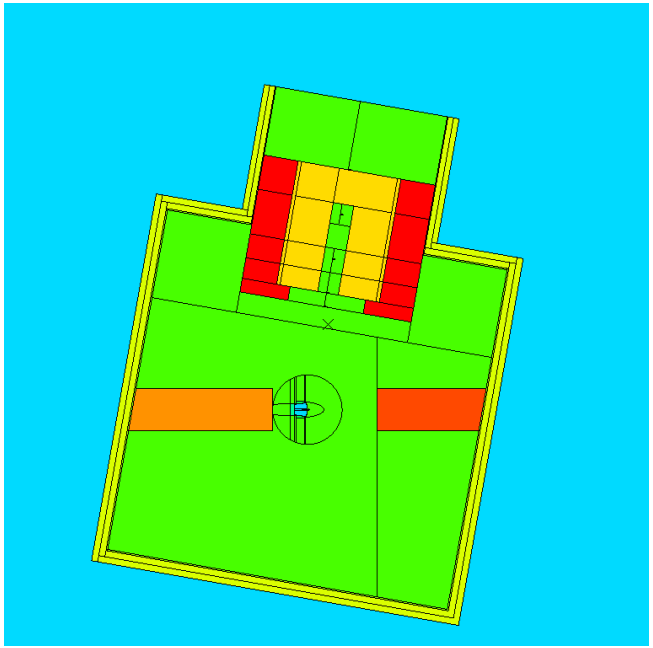

Y=30

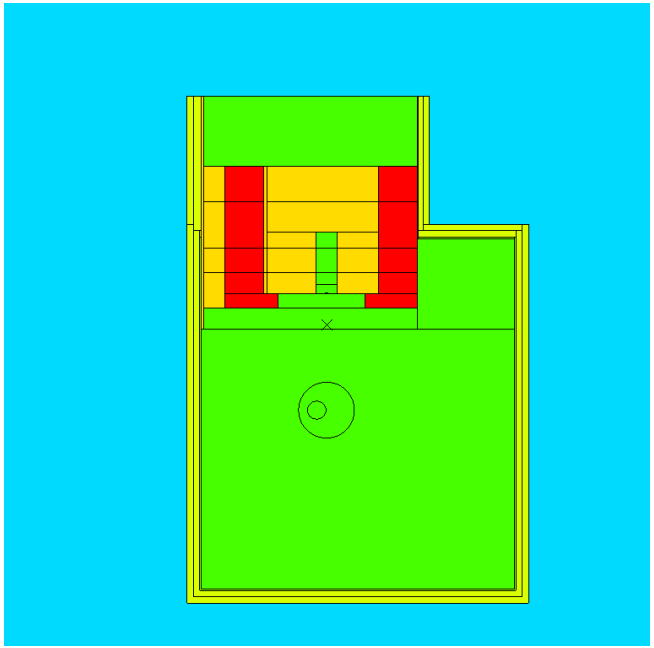

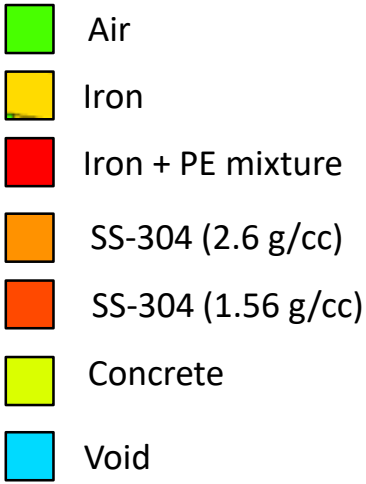

Source definition

Source **cards**

Source definition thanks to keyword ↔ value syntax

Geometrical distribution, angular distribution, energetic distribution, time distribution

Location, energy, direction and time independant

Source **file** (like SSW/SSR card in MCNP-5/6)

Source particles stored in a dedicated file

t, e, x, y, z, u, v, w, w, n

Source **library**

External source provided in a dynamically linked library *source.so*

source(int *ipt, double *x, double *y, double *z, double *u, souble *v, double *w, double *e, double *we, double *t, double *param, double (*randtri)(void))

Necessity to implement source.F90, srcdx.F90, interp.F90, iteg.F90, xint1d.F90, xinterp2d.F90 and probably other source files in source.so

Neutron sources generation

Modification of source.F90 file in MCNP-5

- After applying the patch, a write(6, *) command implementation at the end of the source.F90 file to dump the neutron characteristics

Python script

- A dedicated PYTHON script translation from MCNP output file into the so-called *.stock files storing the neutrons

Source analysis on 10^7 neutrons

10^8 neutrons file
MCNP-5 file → 21 Gb
TRIPOLI-4® file → 16 Gb

FNS Duct experiment – Source analysis

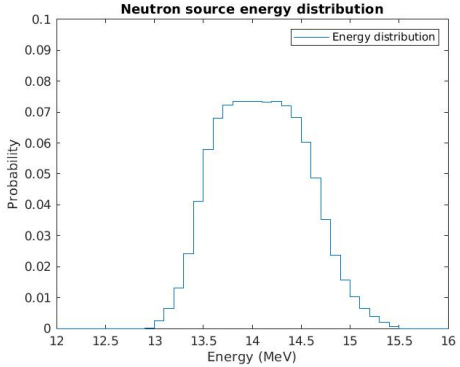

Energy distribution

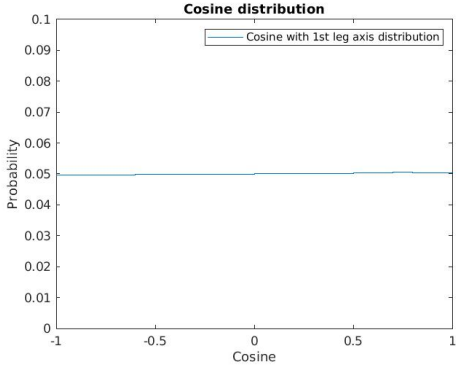

Cosine distribution

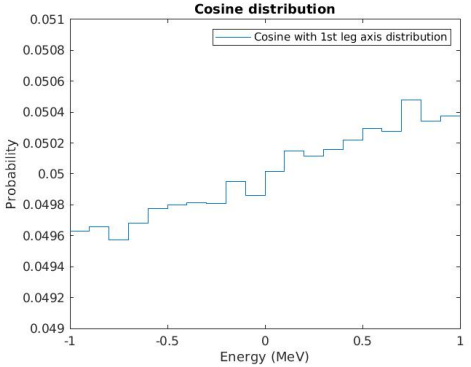

Cosine distribution (fine scale)

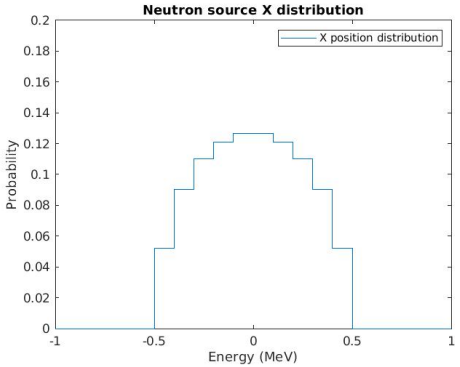

X distribution

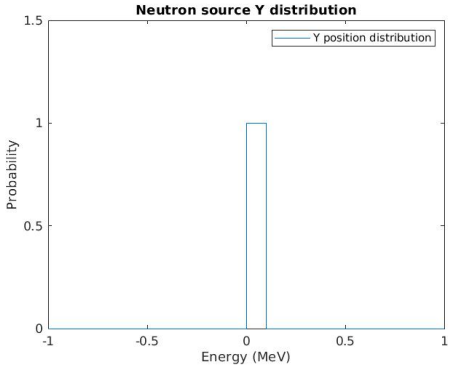

Y distribution

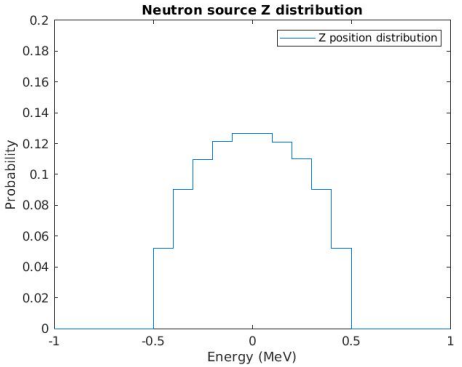

Z distribution

Simulation data

Hardware

Dell Workstation
Intel Xeon Platinum 8270 2.7GHz,(4.0GHz Turbo, 26C, 10.4GT/s 3UPI, 35.75MB Cache, HT (205W) DDR4-2933 2nd)
256Go 8x32Go DDR4 2933 RDIMECC

Code Version

4.11.1 Linux CentOS 7

Simulation options

STORAGE source definition in files (10^7, 10^8 or 10^9 neutrons)
No Probability Tables (^{58}Fe only with PTs between 350 keV and 3 MeV)
Energy cutoff for ^{93}Nb(n, 2n) and ^{115}In(n, n')
No UNIT_BASE_INTERPOLATION
300K temperature

DE LA RECHERCHE À L'INDUSTRIE

Nuclear data

IRFM/SI²P/GISP

Institut de Recherche sur la Fusion par confinement Magnétique

Neutron transport ND

Iron isotopes test mainly: ^{54}Fe, ^{56}Fe, ^{57}Fe, ^{58}Fe

FENDL-2.1

FENDL-3.1d

Isotope	FENDL-2.1	FENDL-3.1d
^{54}Fe	ENDF/B-VI.5	ENDF/B-VII ENDF/B-VI.5 with MF=6 MT=5 modification
^{56}Fe	JEFF-3.0	FENDL-3.0 (JEFF-3.1.1 until 20 MeV and TENDL-2011 above 20 MeV)
^{57}Fe	ENDF/B-VI.4	ENDF/B-VII Based on ENDF/B-VI.4 with MF=6 MT=5 modification
^{58}Fe	ENDF/B-VI.2	JEFF-3.1.1

Neutron dosimetry ND

IRDF-2002

IRDFF-II

```
m11     6012.31c  6.0860e-4  14028.31c  3.6065e-4  $ iron for the assembly
       14029.31c  0.1843e-4  14030.31c  0.1221e-4
       15031.31c  3.0452e-5
       16032.31c  5.5899e-06 16033.31c  4.4122e-08 16034.31c  2.4767e-07  &
       16036.31c  1.1766e-09
       25055.31c  9.0565e-4
       26054.31c  4.8262e-3  26056.31c  7.6320e-2
       26057.31c  1.8306e-3  26058.31c  2.3299e-4
```

Dosimetry reaction rates

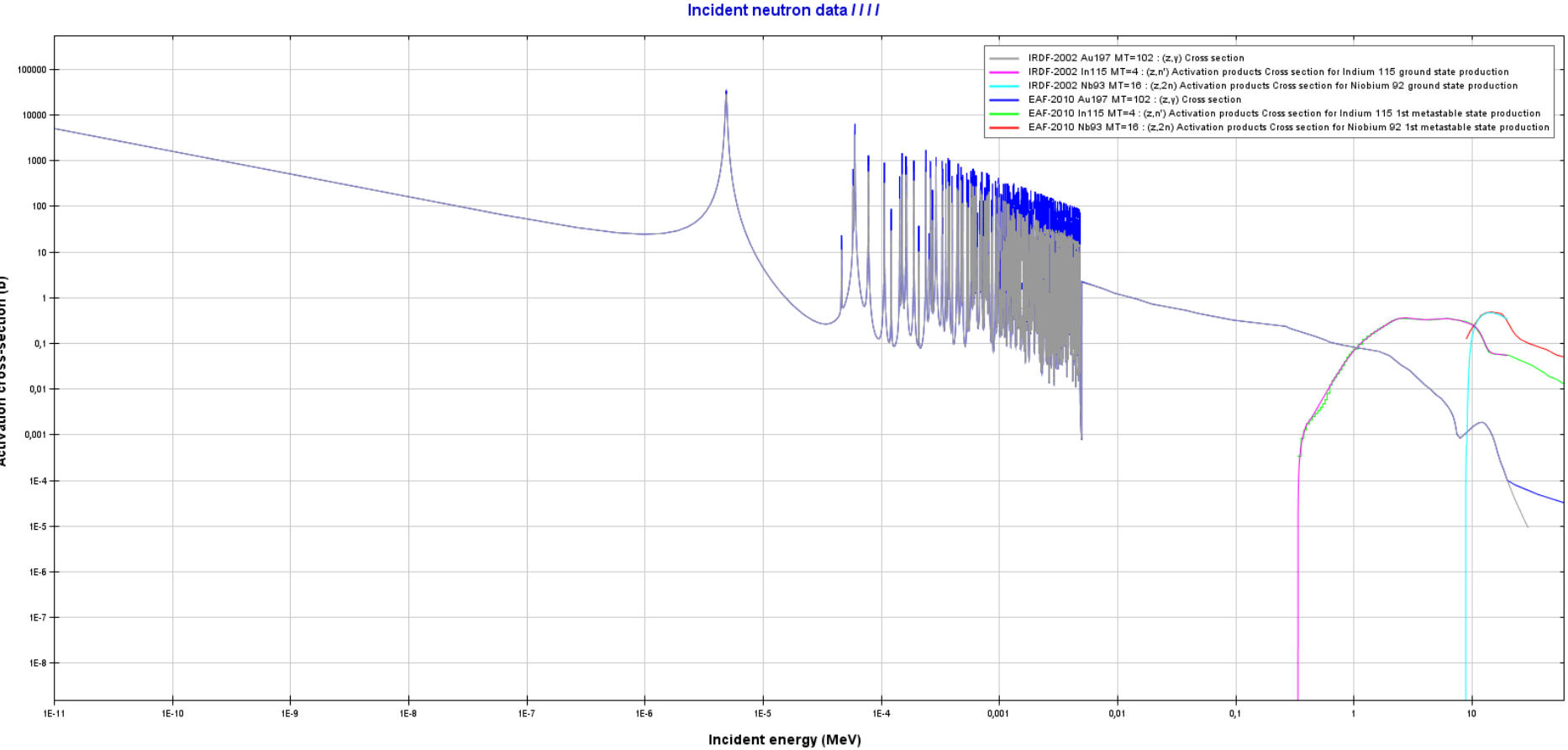

DE LA RECHERCHE À L'INDUSTRIE

Variance reduction techniques

IRFM/SI²P/GISP

Institut de Recherche sur la Fusion par confinement Magnétique

TRIPOLI-4® VRT methods

Exponential Transform

- Legacy TRIPOLI-1, TRIPOLI-2, TRIPOLI-3 and TRIPOLI-4® variance reduction method
- Based on Importance Sampling theory and biased transport process
- Coupled with importance maps for particle weight control
- Requires experience in complex configurations → Particle weight control mandatory

Adaptive Multilevel Splitting

- Based on analog transport process
- Easier to set up → No risk to have the so-called « long history » issue

CADIS methodolgy and Weight Windows implementation to come in version 12

VRT analyses performed with a simplified source (punctual, isotropic, energetic distribution from PYTHON script analysis)

Exponential transform – General considerations

Biased flux equation

$$\phi^*(\vec{r}, v, \vec{\Omega}, t) = \phi(\vec{r}, v, \vec{\Omega}, t) \times I(\vec{r}, v, \vec{\Omega}, t)$$

$\phi \times I$ constant to avoid huge flux attenuation

$I(\vec{r}, v, \vec{\Omega}, t)$ times $\frac{1}{v} \times \frac{\partial}{\partial t}\phi(\vec{r}, v, \vec{\Omega}, t) + \vec{\Omega} \cdot \vec{\nabla}\phi(\vec{r}, v, \vec{\Omega}, t) + \Sigma_t(\vec{r}, v, \vec{\Omega}, t) \times \phi(\vec{r}, v, \vec{\Omega}, t) = C\phi(\vec{r}, v, \vec{\Omega}, t) + S(\vec{r}, v, \vec{\Omega}, t)$

leads to the biased transport equation

$$\frac{1}{v} \times \frac{\partial}{\partial t}\phi^*(\vec{r}, v, \vec{\Omega}, t) + \vec{\Omega} \cdot \vec{\nabla}\phi^*(\vec{r}, v, \vec{\Omega}, t) + \Sigma_t^*(\vec{r}, v, \vec{\Omega}, t) \times \phi^*(\vec{r}, v, \vec{\Omega}, t) = C^*\phi^*(\vec{r}, v, \vec{\Omega}, t) + S^*(\vec{r}, v, \vec{\Omega}, t)$$

Exponential transform – General considerations

$$\phi^*(\vec{r}, v, \vec{\Omega}, t) = \phi(\vec{r}, v, \vec{\Omega}, t) \times I(\vec{r}, v, \vec{\Omega}, t)$$

Biased transport operator

$$\Sigma_t{}^*(\vec{r}, E, \vec{\Omega}) = \Sigma_t(\vec{r}, E, \vec{\Omega}) - \vec{\Omega} \cdot \frac{\vec{\nabla} I(\vec{r}, E, \vec{\Omega})}{I(\vec{r}, E, \vec{\Omega})} = \Sigma_t(\vec{r}, E, \vec{\Omega}) - \vec{\Omega} \cdot \frac{\left\|\vec{\nabla} I(\vec{r}, E, \vec{\Omega})\right\|}{I(\vec{r}, E, \vec{\Omega})} \cdot \frac{\vec{\nabla} I(\vec{r}, E, \vec{\Omega})}{\left\|\vec{\nabla} I(\vec{r}, E, \vec{\Omega})\right\|}$$

$$\Sigma_t{}^*(\vec{r}, E, \vec{\Omega}) = \Sigma_t(\vec{r}, E, \vec{\Omega}) - K \cdot \vec{\Omega} \cdot \overrightarrow{\Omega_0}$$

Biased collision operator

$$\Sigma_s{}^*(\vec{r}, E' \to E, \overrightarrow{\Omega'} \to \vec{\Omega}) = \Sigma_s(\vec{r}, E' \to E, \overrightarrow{\Omega'} \to \vec{\Omega}) \cdot \frac{I(\vec{r}, E, \vec{\Omega})}{I\left(\vec{r}, E', \overrightarrow{\Omega'}\right)}$$

Difficult to implement because of Σ_s definition complexity (Legendre polynomial, Watt spectrum, …)

Biased source

$$Q^*(\vec{r}, E, \vec{\Omega}) = Q(\vec{r}, E, \vec{\Omega}) \cdot I(\vec{r}, E, \vec{\Omega})$$

Exponential transform – General considerations

Importance sampling inspired from the previous biased transport kernel definition

$$\Sigma_t{}^*(\vec{r}, E, \vec{\Omega}) = \Sigma_t(\vec{r}, E, \vec{\Omega}) - K \cdot \vec{\Omega} \cdot \overrightarrow{\Omega_0}$$

And the biased source definition because thanks its consistent with the importance sampling to have weight consistency

$$Q^*(\vec{r}, E, \vec{\Omega}) = Q(\vec{r}, E, \vec{\Omega}) \cdot I(\vec{r}, E, \vec{\Omega})$$

K values automatically provided by TRIPOLI-4® (Placzek equation resolution)

Importance (or weight map) automatically produced by TRIPOLI-4® →Djikstra optimization algorithm

Exponential transform

g1

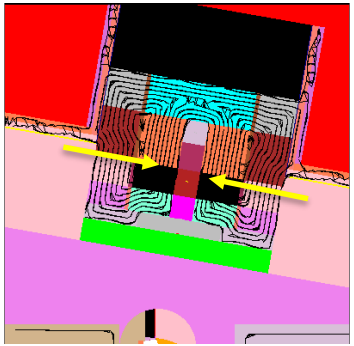

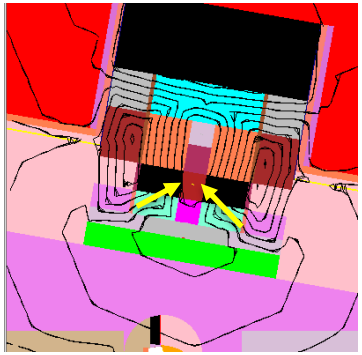

g2

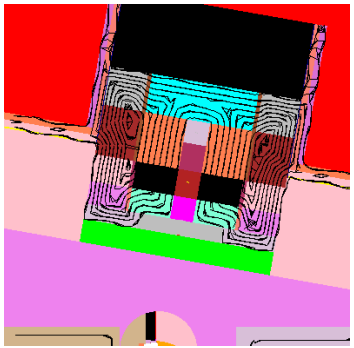

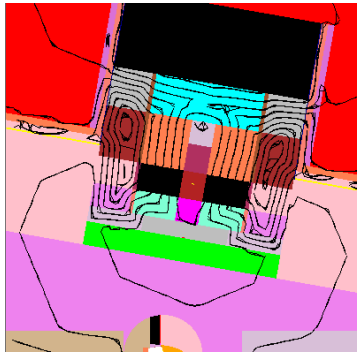

X=0 No VOID option

X=0 VOID option

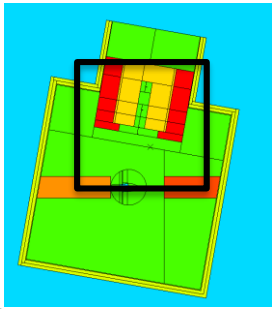

First leg X =0

Because of $\overrightarrow{\Omega_0}$ definition

$$\Sigma_t{}^*(\vec{r}, E, \vec{\Omega}) = \Sigma_t(\vec{r}, E, \vec{\Omega}) - K \cdot \vec{\Omega} \cdot \overrightarrow{\Omega_0}$$

$$K = \frac{\left\|\vec{\nabla} I(\vec{r}, E, \vec{\Omega})\right\|}{I(\vec{r}, E, \vec{\Omega})}$$

Detector (highest importance) is detector #7

Duct opening

Exponential transform

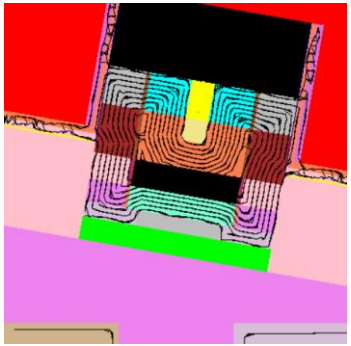

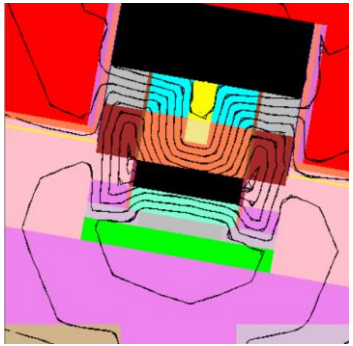

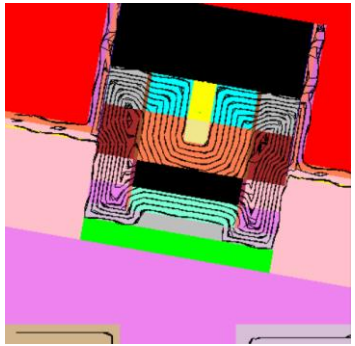

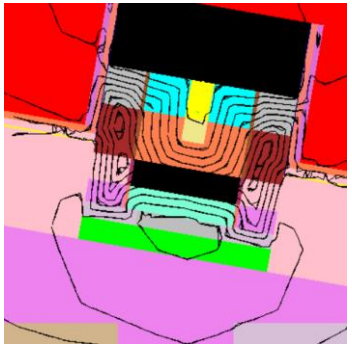

X=-60 No VOID option

X=-60 VOID option

Third leg X = -60

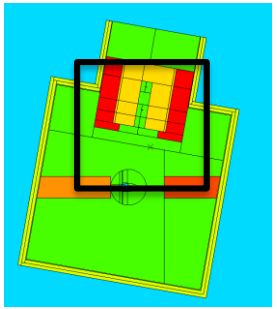

Exponential transform - Results

$$FoM = \frac{1}{\sigma^2 \times t}$$

No optimization
Importance mesh 10 cm

^{93}Nb(n, 2n)

Detector	Analog σ(%)	VOID σ(%)	FoM
#0	0,3	0,2	1,2
#1	0,3	0,2	1,1
#2	0,4	0,3	1,4
#3	0,5	0,3	1,4
#4	6,2	2,2	5,9
#5	22,2	7,7	6,0
#6	16,6	5,1	7,5
#7	42,3	9,6	**14,0**
#8	40,0	8,3	16,9
#9	20,7	10,3	2,9
#10	51,3	10,2	18,2
#11	71,1	25,4	5,7
Time (s)	110716	153805	

^{115}In (n, n')

Detector	Analog σ(%)	VOID σ(%)	FoM
#0	2,5	3,8	1,0
#1	2,9	6,3	0,5
#2	3,4	3,4	2,3
#3	4,3	3,1	4,5
#4	13,4	6,0	11,7
#5	31,4	12,5	14,5
#6	36,8	15,3	13,4
#7	44,2	33,6	**4,0**
#8	66,4	28,6	12,5
#9	45,1	21,9	9,8
#10	84,1	31,7	16,3
#11	93,1	48,3	8,6
Time (s)	4320	1868	

^{197}Au (n, γ)

Detector	Analog σ(%)	VOID σ(%)	FoM
#0	13,2	18,8	2,2
#1	10,8	26,1	0,8
#2	18,0	18,9	4,0
#3	21,4	9,3	23,5
#4	36,6	8,3	86,0
#5	54,8	8,2	198,2
#6	30,6	6,7	93,2
#7	53,6	9,5	**141,7**
#8	63,8	35,5	14,4
#9	42,6	49,4	3,3
#10	23,2	57,0	0,7
#11	48,2	46,5	4,8
Time (s)	99299	22231	

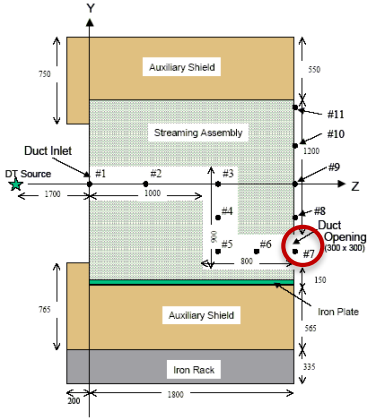

Fig.2 Schematic view of the experimental assembly.

Adaptive Multilevel Splitting

The AMS method consists in:

- performing analog calculations for N particles
- sorting the particles with regard to an importance criteria
- removing some of the particles N1
- splittting some of the particles uniformly amongst the remaining particles
- correcting the simulation weight by the ratio of (N-N1) over N
- iterating the process until N – N1 particles reach the detector

Importance function: distance to origin in the case presented below

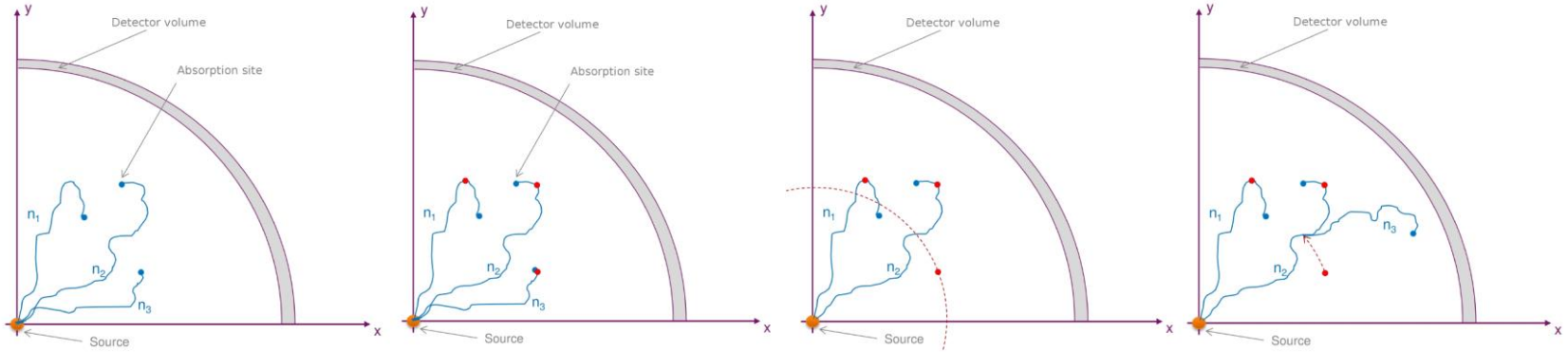

Adaptive Multilevel Splitting

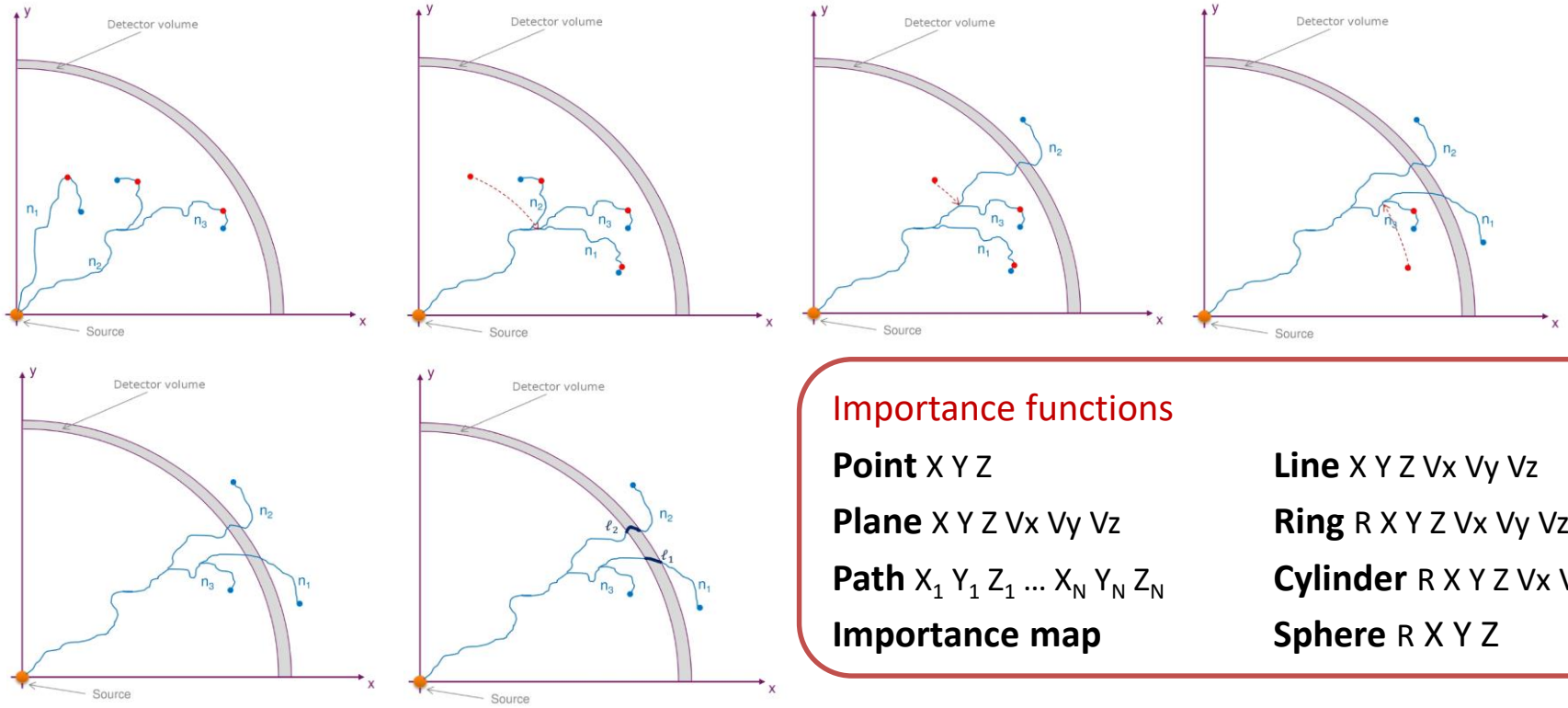

Importance functions

Point X Y Z

Plane X Y Z Vx Vy Vz

Path X_1 Y_1 Z_1 … X_N Y_N Z_N

Importance map

Line X Y Z Vx Vy Vz

Ring R X Y Z Vx Vy Vz

Cylinder R X Y Z Vx Vy Vz

Sphere R X Y Z

AMS - Analyses

^{93}Nb(n, 2n)

Path strength is 1.

$$I = d_{\parallel} - s \times d_{\perp}$$

Detector	Analog σ(%)	Point #7 σ(%)	FoM	Plane σ(%)	FoM	Path σ(%)	FoM
#0	0,3	8,5	0,1	7,7	0,1	7,7	0,1
#1	0,3	9,6	0,1	8,6	0,1	8,8	**0,1**
#2	0,4	12,8	0,1	10,5	0,1	10,8	**0,1**
#3	0,5	17,0	0,1	13,2	0,1	13,0	**0,1**
#4	6,2	8,3	41,2	15,7	8,0	7,7	**43,0**
#5	22,2	32,1	35,5	19,8	64,4	16,8	**114,9**
#6	16,6	15,7	83,2	37,2	10,3	15,2	**79,2**
#7	42,3	10,5	**1210,5**	29,7	**104,0**	14,7	**548,4**
#8	40,0	9,3	1371,9	14,1	**412,3**	14,5	507,4
#9	20,7	13,6	172,8	7,3	**418,6**	19,0	78,5
#10	51,3	48,3	83,8	16,9	**471,2**	55,1	57,4
#11	71,1	57,3	114,4	34,5	**218,3**	51,9	124,3
Time (s)	110716	1491		2159		1672	

Tested options:

- Point
- Plane
- Path

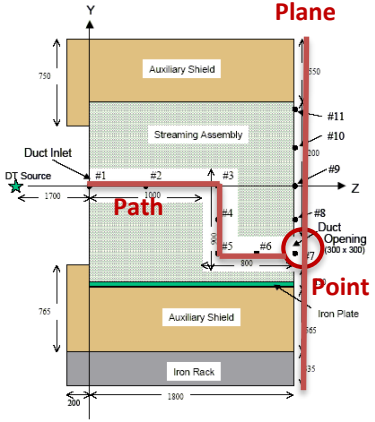

Fig.2 Schematic view of the experimental assembly.

AMS is not efficient for the detectors close to the source: iterations do not bring more contributions BUT simulation time is larger →
2 calculations: ANALOG + AMS to cover all the detectors

AMS - Analyses

^{115}In(n, n')

Detector	Analog σ(%)	Point #7 σ(%)	FoM	Plane σ(%)	FoM	Path σ(%)	FoM
#0	2,5	5,4	0,3	5,5	0,3	5,3	0,3
#1	2,9	5,6	0,3	5,8	0,3	5,4	**0,3**
#2	3,4	6,5	0,3	8,1	0,2	7,3	**0,3**
#3	4,3	7,3	0,4	8,1	0,4	8,6	**0,3**
#4	13,4	4,1	13,7	6,8	5,0	3,5	**17,6**
#5	31,4	13,4	7,0	8,1	19,0	7,2	**23,2**
#6	36,8	7,6	29,7	10,3	16,1	7,2	**31,9**
#7	44,2	10,2	**23,9**	16,3	**9,3**	9,9	**24,6**
#8	66,4	64,4	1,3	11,2	**44,9**	13,0	31,7
#9	45,1	12,7	16,0	6,9	**54,3**	10,8	21,4
#10	84,1	72,0	1,7	16,3	**34,0**	16,7	30,9
#11	93,1	34,7	9,1	29,5	**12,7**	29,1	12,5
Time (s)	4320	3414		3388		3539	

Tested options:

- Point
- Plane
- Path

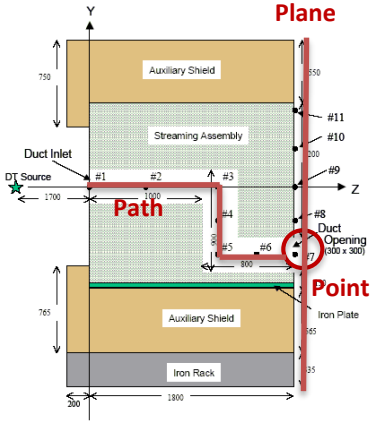

Fig.2 Schematic view of the experimental assembly.

Efficiency decreases but remains interesting with the PLANE option

AMS - Analyses

$^{197}Au(n, \gamma)$

Detector	Analog σ(%)	Point #7 σ(%)	FoM	Plane σ(%)	FoM	Path σ(%)	FoM
#0	13,2	18,5	2,7	79,8	0,3	50,5	**0,5**
#1	10,8	26,8	0,9	35,5	1,0	20,6	**2,0**
#2	18,0	18,1	5,3	68,5	0,7	27,3	**3,1**
#3	21,4	21,2	5,5	34,6	4,1	22,0	**6,8**
#4	36,6	18,5	20,8	57,7	4,3	19,7	**24,8**
#5	54,8	17,3	53,7	34,7	26,8	17,9	**67,7**
#6	30,6	22,4	10,0	21,1	22,7	20,0	**16,8**
#7	53,6	23,9	**26,9**	26,4	**44,3**	25,7	**31,4**
#8	63,8	37,7	15,3	40,3	**26,9**	44,2	15,0
#9	42,6	32,9	8,9	45,8	**9,3**	52,4	4,7
#10	23,2	58,3	0,8	39,7	**3,7**	40,5	2,4
#11	48,2	48,7	5,2	46,2	**11,7**	33,7	14,7
Time (s)	99299	18599		9238		13820	

Tested options:

- Point
- Plane
- Path

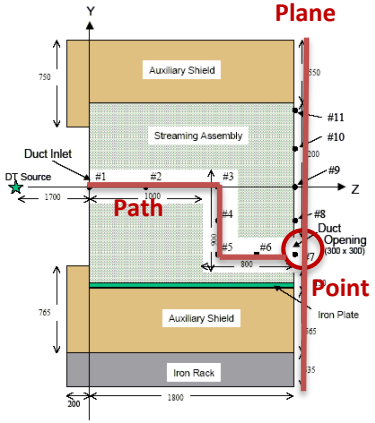

Fig.2 Schematic view of the experimental assembly.

Reason may be the α^n correction weight with large number of iterations for thermal neutrons and small number for high energy neutrons

DE LA RECHERCHE À L'INDUSTRIE

Results

IRFM/SI²P/GISP

Institut de Recherche sur la Fusion par confinement Magnétique

Reaction rates

Calculation normalization

- $^{93}Nb(n, 2n)^{92m}Nb$ calculated reaction rate consistency with the measured value at the duct inlet
- Application to all reaction rates and to neutron flux spectra

Normalization value

From analog calculation with very low variance → FLUX_PT calculation = point flux estimator

Experiment : 1.73E-06 (1 σ = 2,9%)

Analog calculation : 1.12E-06 (1 σ = 0,04%)

Normalization: 1.54

TRACK calculation = track length estimator

1.12E-06 (1 σ = 0.71%)

Source contribution with isotropic assumption in TRIPOLI-4®

Results

Reaction rates

C/E values

Normalization factor: 1.54

Rate	#1	#2	#3	#4	#5	#6	#7	#8	#9	#10	#11
^{93}Nb(n, 2n)	1.02	1.03	0.97	1.47	1.17	X	X	X	1.17	X	X
σ (%) calc	0.9	1.1	1.4	1.8	2.7	6.6	3.9	1.8	0.9	1.8	3.7
^{115}In(n, n')	0.87	0.88	0.97	1.25	1.04	0.91	1.58	X	1.40	X	X
σ (%) calc	0.7	0.8	1.0	0.7	1.1	2.4	1.9	1.6	1.1	1.6	2.2
^{197}Au(n, γ)	1.16	1.01	1.10	1.23	1.20	0.58	1.02	2.19	2.42	2.01	2.45
σ (%) calc	6.1	6.7	4.3	3.9	4.3	3.6	4.1	6.6	5.6	5.2	7.0

Previous MCNP-4 and FENDL-2 calculations already highlighted the overestimation in detectors #4 and #5 for ^{93}Nb and ^{115}In

^{197}Au reaction rates too high with current calculation: detector cell is made of air and gold can absorb neutrons in thermal range and in 6 eV resonance

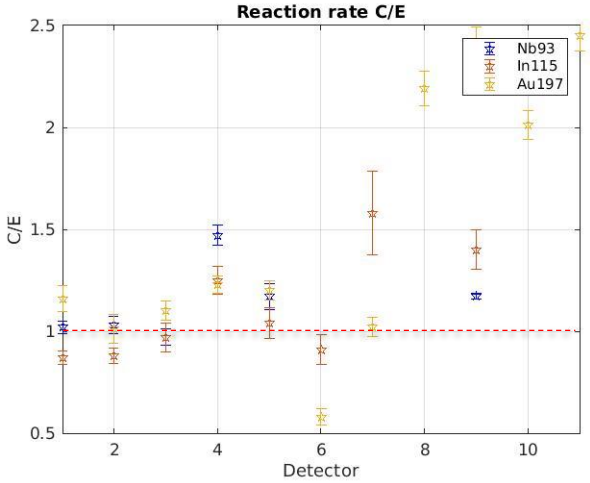

Reaction rates

Normalization factor: 1.54

Calculation and Experiment values comparison

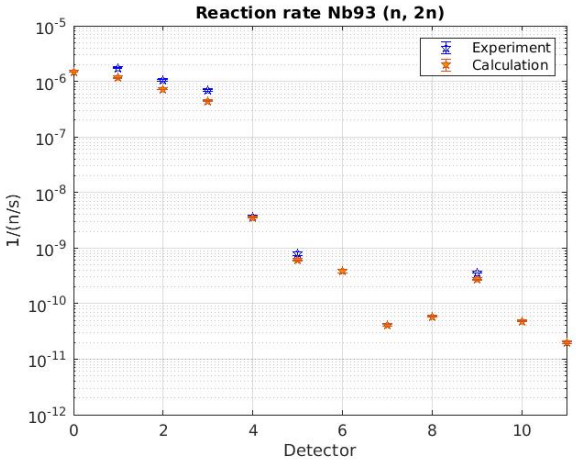

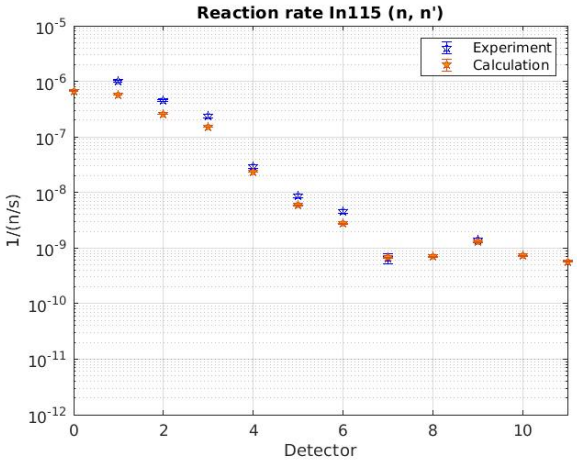

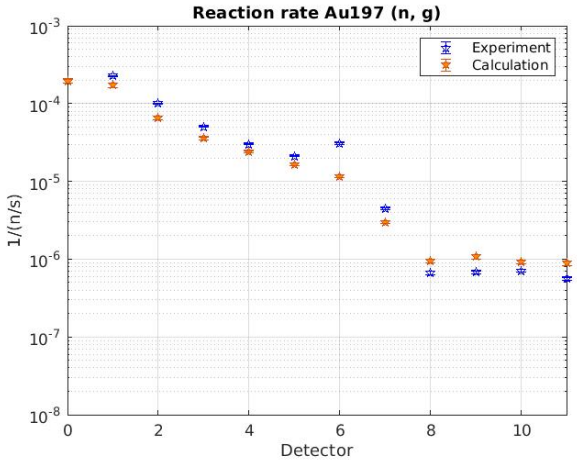

Convergence analyses

^{93}Nb(n, 2n)

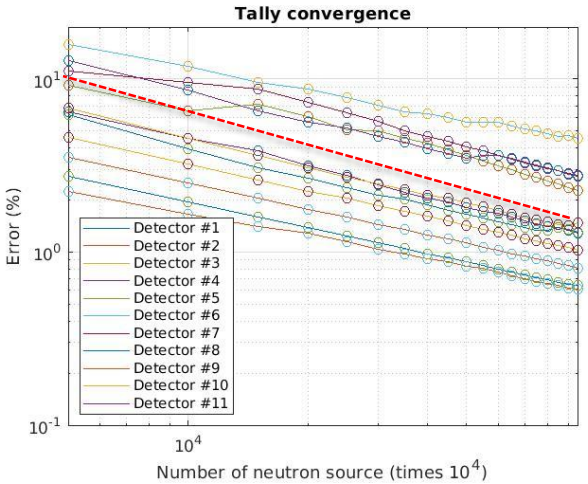

^{115}In(n, n')

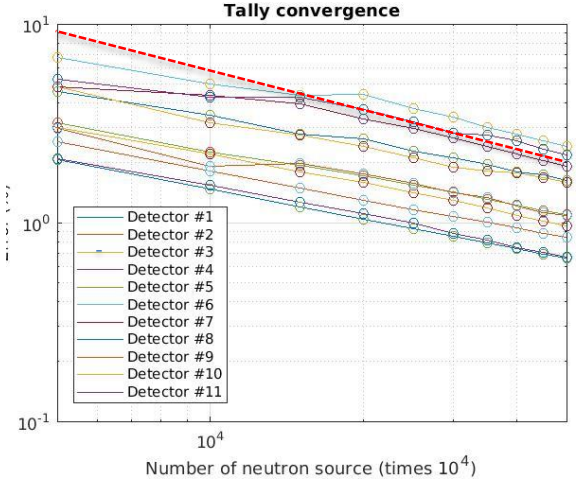

^{197}Au(n, γ)

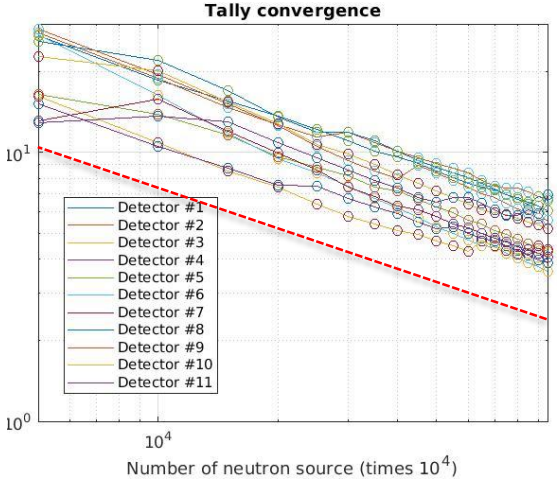

Neutron flux

Difficulty in unfolding of the almost monoenergetic measured data → underestimation already observed

Inconsistency at high energy → not consistent with the neutron spectrum from DT source subroutine

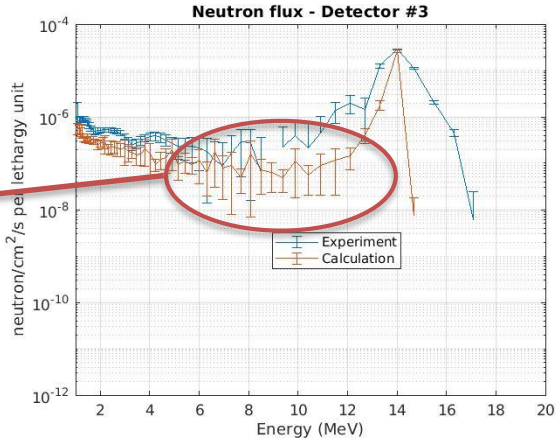

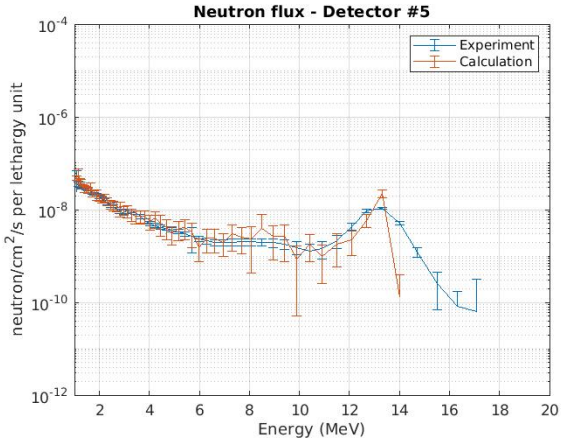

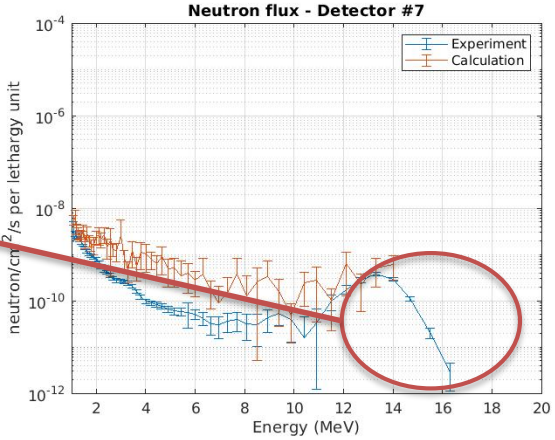

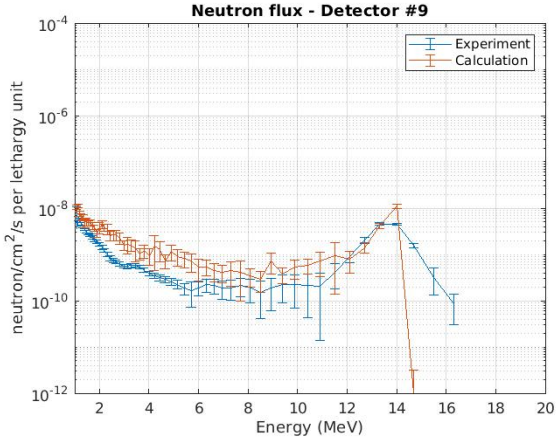

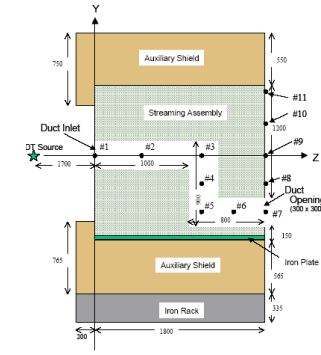

t.2 Schematic view of the experimental assembly.

Reaction rates – ND evaluations

Assuming that $X_{det\#i}^{FENDL-j}$ are independant random variables (all detectors and FENDL-2.1 or FENDL-3.1d)
→ 11 detectors

Detector	^{93}Nb(n, 2n)	^{115}In(n, n')	^{197}Au(n,g)
χ^2_{calc}	9.2	14.7	8.6
$P_{11}(\chi^2 > \chi^2_{calc})$	[0.50, 0.90]	≈0.20	[0.50, 0.90]

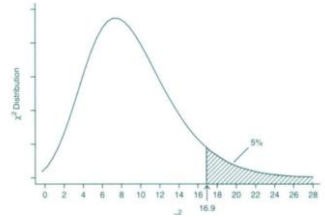

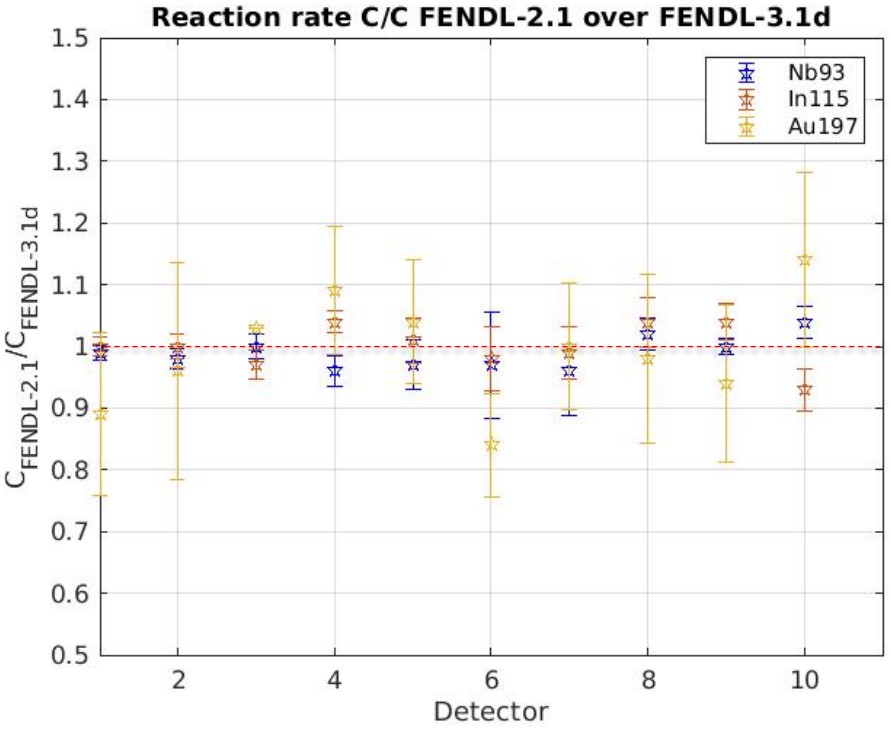

Main results

- Despite the normalization issue, the FNS-Duct benchmark is an interesting configuration with regard to typical fusion reactor configurations with a quite complex transport path

- TRIPOLI-4® and FENDL-3.1d reproduce the experimental results with satisfying accuracy and precision thanks to the VRTs implemented in the code

- Mainly iron cross sections tested (concrete back-scattering probably negligible → could be checked)

- No obvious difference between FENDL-3.1d and FENDL-2.1

- No impact of dosimetry cross section (IRDF-2002 and IRDFF-II) for ^{93}Nb and ^{115}In

Improvements to consider

- More ND comparison required→ FENDL-3.2, JEFF-3.3, JEFF-4.0T1, ENDF/B-VII.1, ENDF/B-VIII.0, TENDL-2021 (check first the changes with regard to the iron XS)
- DT source development – libsource.so → to allow easier calculations and to use for other FNS or FNG benchmark analyses
- AMS convergence results analysis → A better confidence is the error estimation
- Sensitivity analyses → To highlight to which ND and to which energy domain the calculation results are sensitive
- MCNP-5/6 comparative analyses → To assess the code options impact (ACE format, neutron simulation options like Unit Base for instance)

Thank you for your attention

DE LA RECHERCHE À L'INDUSTRIE

IRFM I SI²P I GISP

Institut de Recherche sur la Fusion par confinement Magnétique